Growth, characterization and nonlinear optical activities of some chalcones derivatives

Shaik Alla Nazeer[1], D. Ramasamy[2], J. Anandakumaran[1], G. Ramasamy[1,2] *

[1]Department of Chemistry, Annamalai University, Annamalai Nagar 608002, India

[2]Department of Chemistry, Government Thirumagal Mills College, Gudiyattam, Vellore Dt. Tamilnadu 632602

Abstract:

The growth and characterization of NLO active chalcone derivatives, 1-(4-chlorophenyl)-3-(4-nitrophenyl) prop-2-en-1-one (4CPNPC), 1-(4-chlorophenyl)-3-(4-methoxyphenyl) prop-2-en-1-one (4CPMPC) and 3-(3-chlorophenyl)-1-(4-methoxyphenyl) prop-2-en-1-one (3CPMPC) are grown by slow evaporation solution growth technique from ethanolic solution at room temperature. Single crystal XRD analysis reveals that 4CPNPC and 4CPMPC belong to the orthorhombic system with noncentrosymmetric space group $P\text{na}2_1$ whereas 3CPMPC crystallizes in monoclinic system with noncentrosymmetric space group $P2_1$. The band gap energies of the specimens were estimated by the DRS data using Kubelka – Munk algorithm. Good thermal stability up to the melting point is observed. SEM images reveal imperfections, voids and surface roughness. It is interesting to observe that when Cl- and -OCH_3 groups are in *para*- position enhanced SHG activity is observed because of facile charge transfer. Theoretical calculations were performed to derive the optimized molecular structure, HOMO – LUMO diagram and first-order molecular hyperpolarizability.

Keywords: Crystal growth, Optical properties, chalcones derivatives, Band-gap energy, nonlinear optical property

Introduction:

Chalcones and their analogues are relatively easily available, not only by isolation from natural products but also by the methods of classical and combinatorial synthesis. The cytotoxic, anticancer, chemopreventative and mutagenic properties of a number of chalcones have been reviewed [1]. Chalcones and their analogues are used as potential therapeutic agents in diseases of the cardiovascular system and their heterocyclic analogues exhibit anti-inflammatory, antitumour, antibacterial, antifungal, antitubercular, antiviral, antiprotozal and gastro protective activities [2]. In addition, with appropriate substituents, chalcones are a class of NLO materials [3,4]. Recently, it has been noted that, among many organic compounds reported for their second harmonic generation, chalcone derivatives have excellent blue light transmittance and good crystallizability. Among the many known organic NLO materials, chalcones exhibit extremely high and fast nonlinearity and show a preference to crystallize as noncentrosymmetric structures [5-7]. Another importance of this type of compound is their high photosensitivity and thermal stability which are used in developing various crystalline electro-optical devices [8,9]. Recently, our team investigated the synthesis, growth, structure and quantum mechanical studies of some chalcone derivatives 10-15]. In the present investigation, we report the growth and characterization of NLO active chalcone derivatives, 1-(4-chlorophenyl)-3-(4-nitrophenyl)prop-2-en-1-one (4CPNPC), 1-(4-chlorophenyl)-3-(4-methoxyphenyl)prop-2-en-1-one (4CPMPC) and 3-(3-chlorophenyl)-1-(4-methoxyphenyl)prop-2-en-1-one (3CPMPC) using single crystal XRD, powder XRD, FT-IR, UV-vis, TG/DTA, SEM, SHG and theoretical studies.

1. Experimental

Synthesis and crystal growth

The compounds 4CPNPC, 4CPMPC and 3CPMPC were synthesized by mixing stoichiometric amounts of acetophenone (4-chloroacetophenone, 4-methoxyacetophenone) with appropriate benzaldehyde (4-nitrobenzaldehyde, 4-methoxybenzaldehyde and3-chlorobenzaldehyde) in the molar ratio of 1:1. The reactants were dissolved in ethanol, thoroughly mixed using a magnetic stirrer (10 minutes) and 20 % NaOH solution was added drop by drop at 25° C[147] for 30 minutes. After stirring for 3 hours the contents of the flask were poured into ice-cold water. The resulting crude solid was collected by filtration, dried and purified by

recrystallization process using ethanol as a solvent. Purity of the compounds was improved by recrystallization process using ethanol as a solvent.

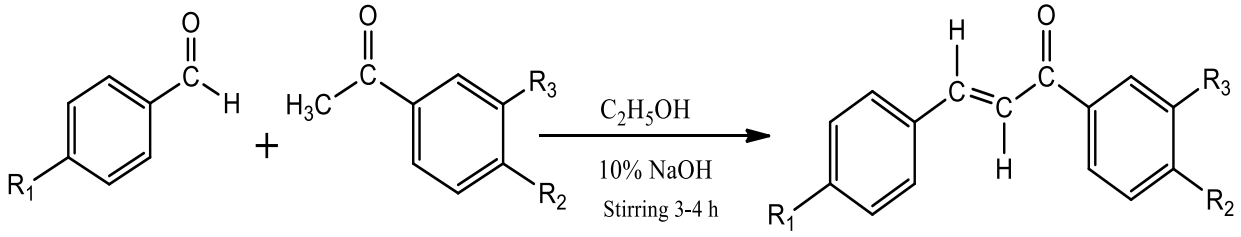

where	4CPNPC	4CPMPC	3CPMPC
R_1	NO_2	OCH_3	OCH_3
R_2	Cl	Cl	H
R_3	H	H	Cl

Characterization

In order to ascertain the structure, purity and identification of the grown crystal, single crystal X-ray diffraction data were collected with a specimen 0.35 x 0.30 x 0.30 mm^3 cut out from the grown crystals using an Oxford Diffraction Xcalibur-S CCD system equipped with graphite monochromated Mo*Kα*(λ=0.71073 Å) radiation at 293 K. The structure was solved by direct methods (SHELXS-97) and refined by full-matrix least squares against F^2 using SHELXL-97 software **[16]**.The molecular structure was drawn using ORTEP-3. The powder XRD analysis was performed by using Philips Xpert Pro Triple-axis X-ray diffractometer. The XRD data are analyzed by Rietveld method with RIETAN-2000. The FT-IR spectrum of grown crystals were recorded in the range 4000-400 cm^{-1} using AVATAR 330 FT-IR by KBr pellet technique. The UV-vis analysis was carried out between 200 and 800 nm using the Perkin Elmer Lambda 35 model spectrophotometer. The second harmonic generation test on the crystals was performed by the Kurtz powder SHG method **[17]**.

FT-IR

The FT-IR spectra of 4CPNPC, 4CPMPC and 3CPMPC are shown in **Figs. 2(a) – 2(c).** The C=O stretching frequencies appeared at 1658, 1654 and 1664 cm^{-1} for 4CPNPC, 4CPMPC and 3CPMPC specimens respectively. The assignments of vibrational patterns of 4CPNPC, 4CPMPC and 3CPMPC are listed in **Table 1.**

. Powder and single crystal XRD analyses

The powder XRD patterns of 4CPNPC, 4CPMPC and 3CPMPC specimens show that the samples are of single phase without any detectable impurity. Narrow peaks indicate the good crystallinity of the materials. The powder XRD patterns of the specimens are shown in **Fig. 3.** Single crystal XRD analysis reveals that 4CPNPC and 4CPMPC specimens belong to the orthorhombic system with noncentrosymmetric space group $Pna2_1$ whereas 3CPMPC crystallizes in monoclinic system with noncentrosymmetric space group $P2_1$. The obtained unit cell parameters of 4CPNPC, 4CPMPC and 3CPMPC are in good agreement with the reported values of structural determination Table 2 [18 – 23].

Optical studies

The UV-vis spectra of 4CPNPC, 4CPMPC and 3CPMPC are shown in **Figs. 4(a) to 4(c)** and the cut-off wavelength is ~460 nm. Absorption is minimum in the visible region. Because of high transparency, these specimens are quite useful for optical device applications The band gap energies of the specimens are estimated by the application of Kubelka–Munk formulae[156]. The direct band gap energies of the specimens are deduced as 2.82, 2.88 and 2.90 eV for 4CPNPC, 4CPMPC and 3CPMPC respectively **(Fig. 5).**

Thermal analysis

The recorded TG/DTA spectra of 4CPNPC, 4CPMPC and 3CPMPC are shown in **Figs. 6(a) – 6(c).** In DTA, the sharp endothermic peaks found at ~163, 113 and ~123 °C are assigned to the melting points of 4CPNPC, 4CPMPC and 3CPMPC respectively. Below this endotherm, no exothermic or endothermic peak is observed. In TG, the materials exhibit single-stage weight losses starting around 290, 280 and 240 °C in 4CPNPC, 4CPMPC and 3CPMPC respectively. The sharpness of the endothermic peak observed in DTA shows the good degree of crystallinity of the material. Absence of decomposition up to the melting point ensures the stability of the material for applications in laser technology where the crystals are required to withstand high temperatures. The sharp endotherm is indicative of solid-state transition for relatively pure material.

SEM

The SEM micrographs at different magnifications of the as-grown 4CPNPC, 4CPMPC and 3CPMPC are shown in **Fig. 7.** Crystal imperfections, voids and surface roughness are observed.

SHG efficiency

The SHG test was performed by Kurtz powder method. An Nd:YAG laser with a modulated radiation of 1064 nm was used as an optical source and directed on the powder samples through a filter. The as - grown crystals were ground to a uniform particle size of 125-150 μm and then packed in a microcapillary of uniform bore and exposed to laser radiation at 5.1 mJ/pulse. The SHG efficiencies of all the specimens are listed in **Table 3** and it is seen that the SHG efficiency of 4CPMPC is ~3 times of urea and the efficiency of 3CPMPC is almost equal to that of urea. Our results are in tune with reported higher SHG activity for 4CPMPC[180]. 4CPNPC shows less activity than urea but the green light emission clearly classifies this material as NLO active. It is interesting to observe that when Cl- and -OCH_3 groups are in *para*- position the SHG activity is high while one group (-Cl) is in *meta*-position the activity is considerably reduced. It could be due to the facile change transfer. The SHG activity originates from strong donor acceptor groups and D-π-A type molecule. Substitution of $–NO_2$ group instead of -OCH_3 further reduces the activity significantly. It is a clear demonstration that by tuning the electronic properties the NLO activities can be influenced.

Theoretical studies

The optimized molecular structures of 4CPNPC, 4CPMPC and 3CPMPC are given in **Figs. 8(a) – 8(c).** The calculated polarizability (α), hyperpolarizability (*β),* dipolemoment (μ) and HOMO – LUMO energies for 4CPNPC, 4CPMPC and 3CPMPC of the specimens are listed in **Table 4.** The maximum β is due to the behavior of nonzero μ values.

We have investigated the growth and NLO- activities of many chalcones. Mostly they crystallize in centrosymmetric space groups **(Table 5).** Interestingly, all have high hyperpolarizability *(β)* values and since they crystallize centrosymmetrically, SHG activity is zero. To sustain nonlinearity in the macro level is a challenging problem in the studies of chalcones. But in the present investigation, all the chalcone have high β values and crystallize in noncentrosymmetric space groups, sustaining NLO activity in the macro level. Interestingly, the β value of 4CPMEC is higher than other chalcones in tune with its high SHG activity. **Figs. 9 and 10** show the highest occupied molecular orbital (HOMO) and lowest unoccupied molecular orbital (LUMO) of 4CPMPC and 3CPMPC. The frontier orbital gap facilitates in characterizing the chemical reactivity and kinetic stability of the molecule. The red and green colors represent the positive and negative values for the wave function.

The HOMO is the orbital that primarily acts as an electron donor and the LUMO is the orbital that mainly acts as an electron acceptor. Lower energy gap E_g in the case of 4CPMPC justifies the high β value.

Conclusion

Transparent yellow crystals of NLO active chalcone derivatives, 1-(4-chlorophenyl)-3-(4-nitrophenyl)prop-2-en-1-one, 1-(4-chlorophenyl)-3-(4-methoxyphenyl)prop-2-en-1-one and 3-(3-chlorophenyl)-1-(4-methoxyphenyl)prop-2-en-1-one are grown by slow evaporation solution growth technique from ethanolic solution at room temperature. Single crystal XRD analysis reveals that 4CPNPC and 4CPMPC belong to the orthorhombic system with non centrosymmetric space group $Pna2_1$ whereas 3CPMPC crystallizes in monoclinic system with non centrosymmetric space group $P2_1$. The band gap energies of the specimens were estimated by the DRS data using Kubelka – Munk algorithm. Good thermal stability up to the melting point is observed. SEM images reveal imperfections, voids and surface roughness. It is interesting to observe that when Cl- and $-OCH_3$ groups are in *para*- position enhanced SHG activity is observed because of facile charge transfer. Theoretical calculations were performed to derive the optimized molecular structure, HOMO – LUMO diagram and first-order molecular hyperpolarizability.

References

[1] J.R. Dimmock, D.W. Elias, M.A. Beazely and N.M. Kandepu, *Curr. Med. Chem.*, **1999,** *6*, 1125.

[2] V. Opletalova and D. Sedivy, *Cesk. Farm,* **1999,** *48,* 252.

[3] D. Fichou, T. Watanabe, T. Takeda, S. Miyata, Y. Goto and M. Nakayama, *Jpn. J. Appl. Phys.*, **1988**, *27*, 429.

[4] Y.Goto, A. Hayashi, Y. Kimura and M. Nakayam, *J. Cryst. Growth,* **1991**, *108*, 688.

[5] Ashok Kumar Singh, G. Saxena, R. Prasad and A. Kumar, *J. Mol. Struc.*, **2012,** *1017,* 26.

[6][133] A.Jayarama, H.J.Ravindra, A.P.Menezes,S.M.Dharmaprakash and S. Weng Ng, *J. Mol. Struc.*, **2013,** *1051*, 285.

[7] P.S. Patil, M.S. Bannur, D.B. Badigannavar and S.M. Dharmaprakash, *Opt. Laser Tech.*, **2014,** *55*, 37.

[8] A. Phrutivorapongkul, V. Lipipun, N. Ruangrungsi, K. Kirtikara, K. Nishikawa, S. Maruyama, T. Watanabe and T. Ishikawa, *Chem.Pharm.Bull.*, **2003**, *51*,187.

[9] D. Williams, Nonlinear Optical Properties of Organic and Polymeric, Materials, Washington, DC: *Am. Chem. Soi.,* **1983**.

[10] K. Vanchinathan, G. Bhagavannarayana, K. Muthu and S.P. Meenakshisundaram, *Physica B*, **2011,** *406*, 4195.

[11] M. Rajasekar, K. Muthu, G. Bhagavannarayana and S.P. Meenakshisundaram, *J. Appl. Crystallogr*., **2012,** *45*, 920.

[12] S. Sudha, N. Sundraganesan, K. Vanchinathan, K. Muthu and S.P.Meenakshisundaram, *J. Mol. Struct.,* **2012**, 1030, 191.

[13] S. Sudha, N. Sundraganesan, K. Vanchinathan, K. Muthu and S.P. Meenakshisundaram, *Mol. Simulation*, **2013,** *39*, 330.

[14] V. Meenatchi, K. Muthu, M. Rajasekar and SP. Meenakshisundaram, *Physica B*, **2013,** *419*, 95.

[15] V. Meenatchi, K. Muthu, M. Rajasekar and SP. Meenakshisundaram, *Spectrochim. Acta, Part A,* **2014**, *120,* 72.

[16] Sheldrick, G. M. SHELXL-97, Program for Crystal Structure Solution and Refinement, Release 97-2. University of, Gottingen, Gottingen Germany. **1997.**

[17] Kurtz, S. K.; Perry.T. T. A Powder Technique for the Evaluation of Nonlinear Optical Materials, *J. Appl. Phys.* **1968,***39,* 3798-3813.

[18] V. Meenatchi, K. Muthu, M. Rajasekar and SP. Meenakshisundaram, *Spectrochim. Acta, Part A,* **2014**, *124,* 423.

[19] V. Meenatchi, K. Muthu, M. Rajasekar, G. Bhagavannarayana and SP. Meenakshisundaram, *Optik*, **2014** (Ref. 13-1151).

[20] V. Meenatchi, K. Muthu, M. Rajasekar and SP. Meenakshisundaram, *Optik*, **2014** (Ref. 13-1392).

[21] T. S. Yamuna, H. S. Yathirajan, J.P. Jasinski, A.C. Keeley, B. Narayana and B. K. Sarojini, *Acta Crystallogr. Sec. E,* **2013,** 69, o790.

[22] W.T. A. Harrison, H. S. Yathirajan, B. K. Sarojini, B. Narayana and J. Indira, *Acta Crystallogr. Sec. E,* **2006,** 62, o1647.

[23] N. Ahmad, H. L. Siddiqui, M. Zia-ur-Rehman and M. Parvez, *Acta Crystallogr. Sec. E,* **2010,** 66, o1346.

Table 1 FT-IR frequencies (cm^{-1})

Assignments of vibrations	4CPNPC	4CPMPC	3CPMPC
C=O stretching	1658	1654	1664
C=C stretching	1600	1595	1602
C-H stretching	3062	3064	3064
C-Cl stretching	750	748	777
C-NO_2 asymmetric stretching	1531	-	-
C-NO_2 symmetric stretching	1346	-	-

Table 2. System, space group and cell parameters of 4CPNPC, 4CPMPC and 3CPMPC

Crystal	System/ space group	a/(Å)	b/(Å)	c/(Å)	Volume /($Å^3$)
4CPNPC	Orthorhombic/ *P*na2_1	42.731(2)	5.915(4)	5.017(1)	1293.21
4CPMPC	Orthorhombic/ *P*na2_1	12.830(12)	24.979 (03)	4.025(21)	1291.23
3CPMPC	Monoclinic/ *P*2_1	10.382(3)	3.932(3)	16.870(2)	651.02

Table 3. SHG output

Input beam energy (mJ/pulse)	$I_{2\omega}$/mV	
	Urea	Compounds
1.4	54.8	30 (4CPNPC)
5.1	104	302 (4CPMPC)
5.1	104	102 (3CPMPC)

Table 4. The calculated β components, β_{tot} value (esu), dipole moment (D), α (esu) and HOMO – LUMO (eV) for 4CPNPC, 4CPMPC and 3CPMPC

Components	4CPNPC	4CPMPC	3CPMPC
β_{xxx}	2632.513	-3601.275	-847.704
β_{xxy}	652.746	1847.065	-1393.810
β_{xyy}	272.938	27.929	-224.106
β_{yyy}	40.075	-12.270	-173.841
β_{xxz}	-22.167	57.872	-1.821
β_{xyz}	10.961	11.598	-4.749
β_{yyz}	12.461	-0. 594	1.331
β_{xzz}	-5.783	36.598	36.807
β_{yxx}	-6.289	15.773	-6.489
β_{zzz}	-0.021	9.640	0.0
β_{tot} ($\times 10^{-30}$)	25.743	34.489	16.273
α	31.967	32.608	31.350
μ	2.694	5.087	1.653
E_{HOMO}	-7.074	-5.904	-6.204
E_{LUMO}	-3.102	-2.068	-2.149
E_{HOMO} - E_{LUMO}	3.972	3.836	4.054

Table 5. Hyperpolarizability values of some chalcone derivatives

Compound	β ($x10^{-30}$) (in esu)	Ref
1,5-diphenylpenta-1,4-dien-3-one	7.521	139
1,5-diphenylpenta-2,4-dien-1-one	7.077	173
(2E,6E)-2-(4-bromobenzylidine)-6-(4-methoxy benzylidine)cyclohexanone	7.611	Unpublished results
3-(4-fluorophenyl)-1-(4-methylphenyl)prop-2-en-1-one	14.254	Unpublished results

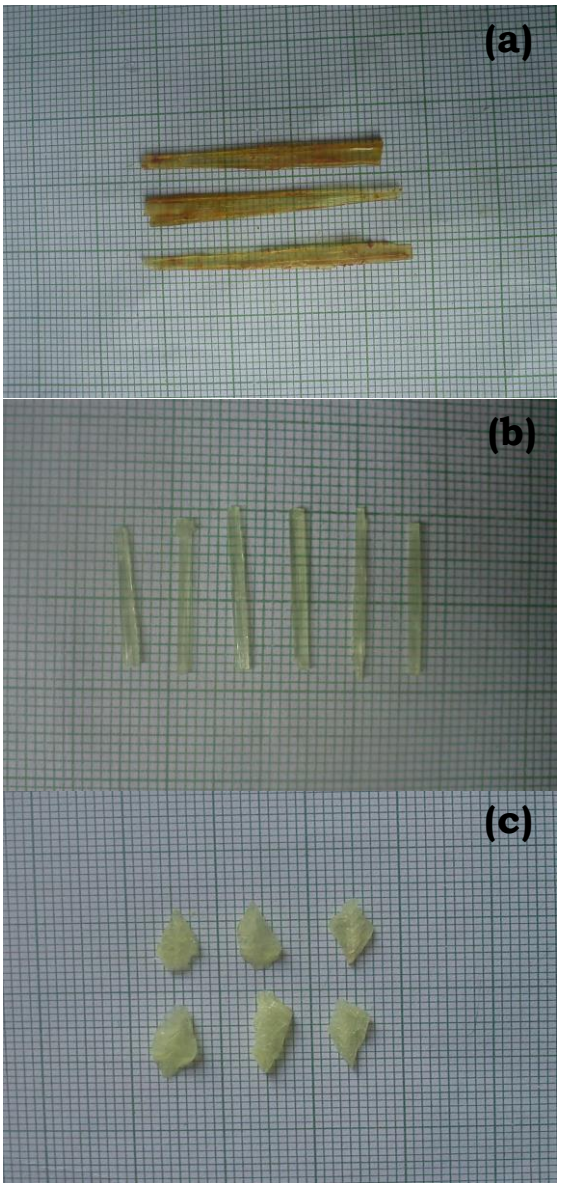

Fig.1. Photographs of as – grown (a) 4CPNPC (b) 4CPMPC and (c) 3CPMPC crystals

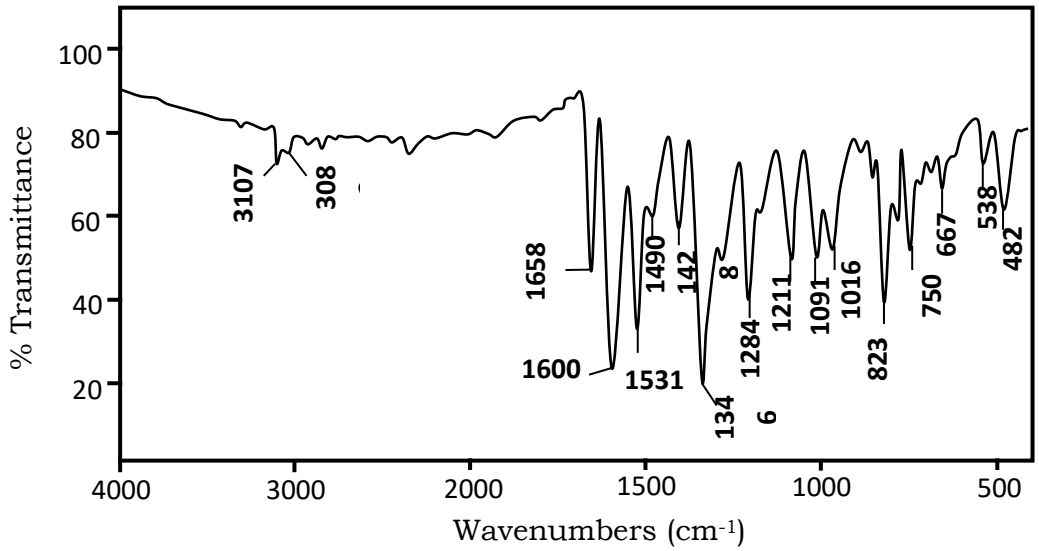

Fig. 2(a). FT-IR spectrum of 4CPNPC

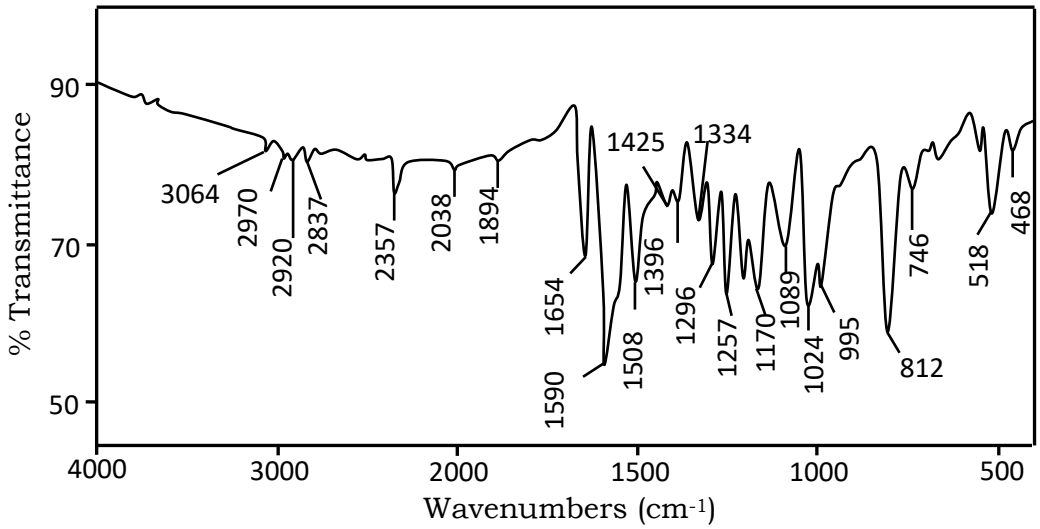

Fig. 2(b). FT-IR spectrum of 4CPMPC

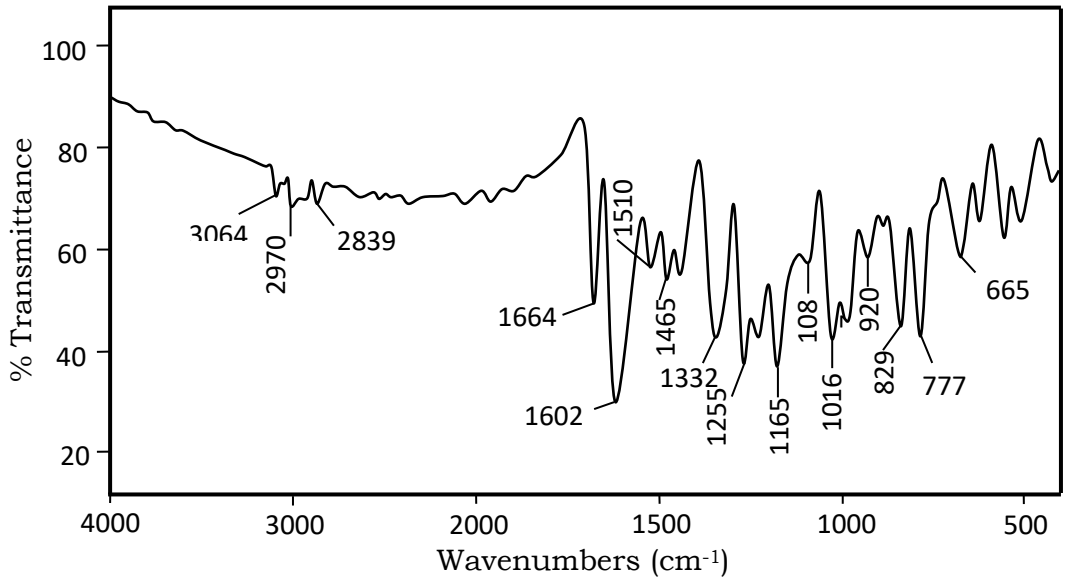

Fig. 2(c). FT-IR spectrum of 3CPMPC

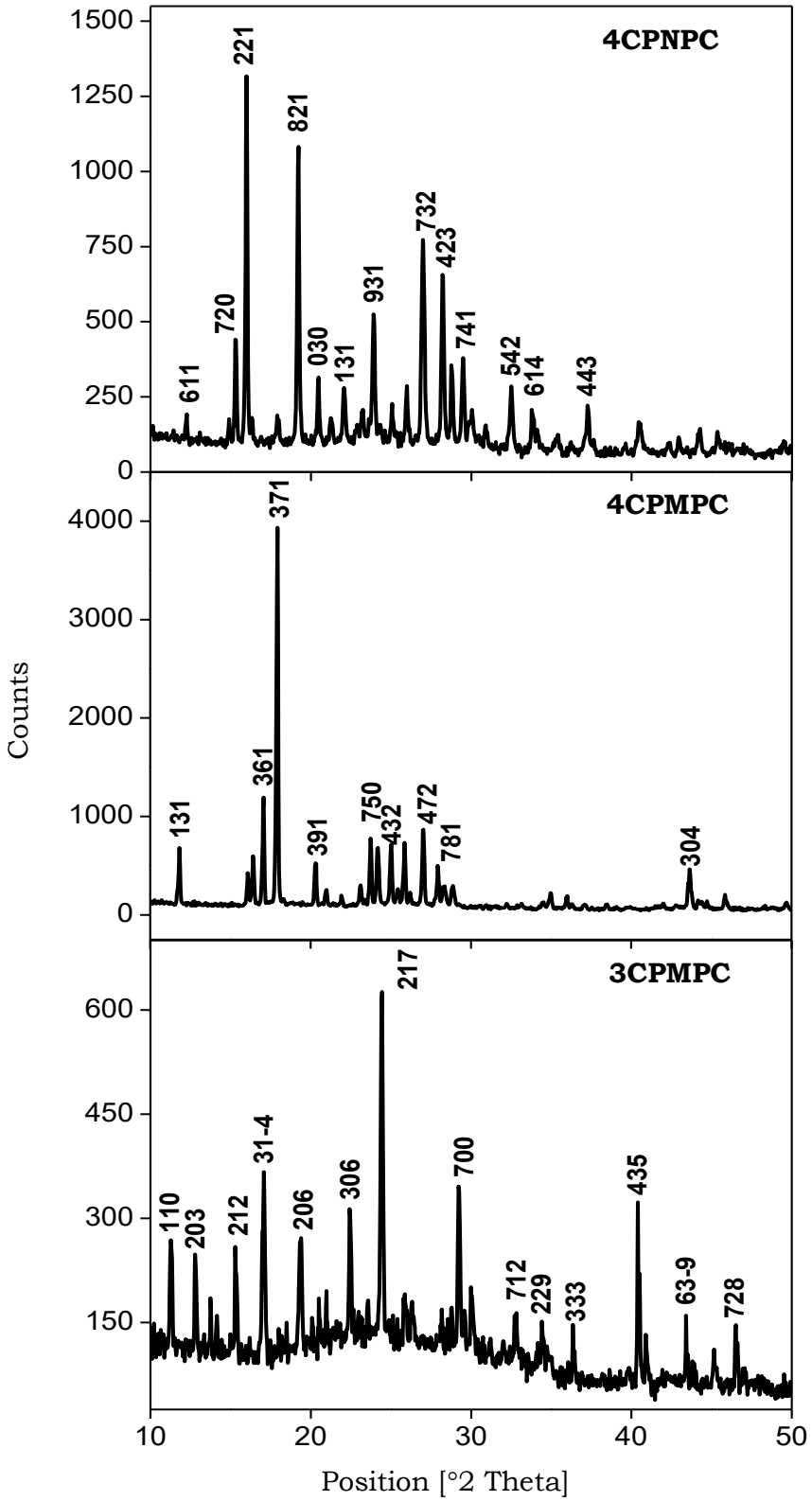

Fig. 3. Powder XRD patterns

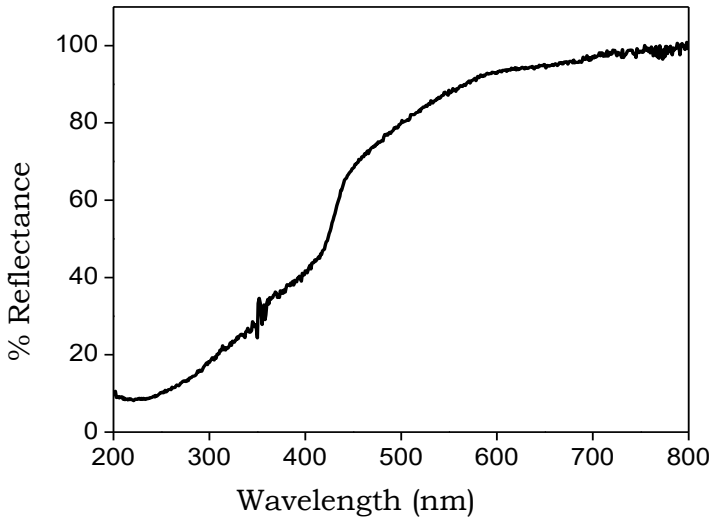

Fig. 4 (a). UV-vis spectrum of 4CPNPC

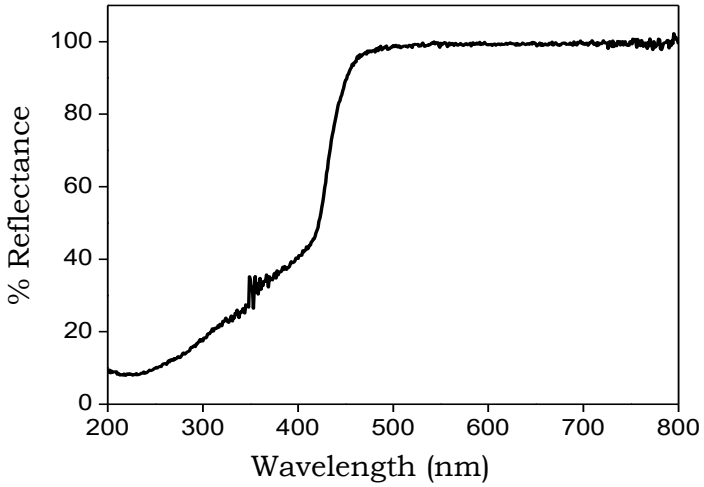

Fig. 4 (b). UV-vis spectrum of 4CPMPC

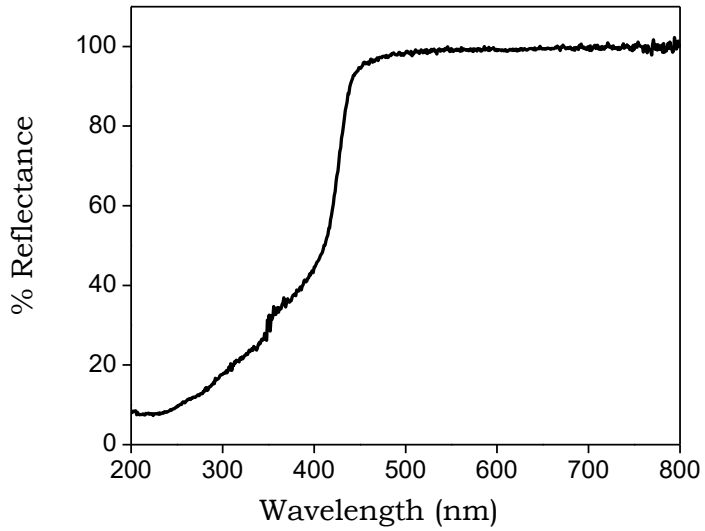

Fig. 4 (c). UV-vis spectrum of 3CPMPC

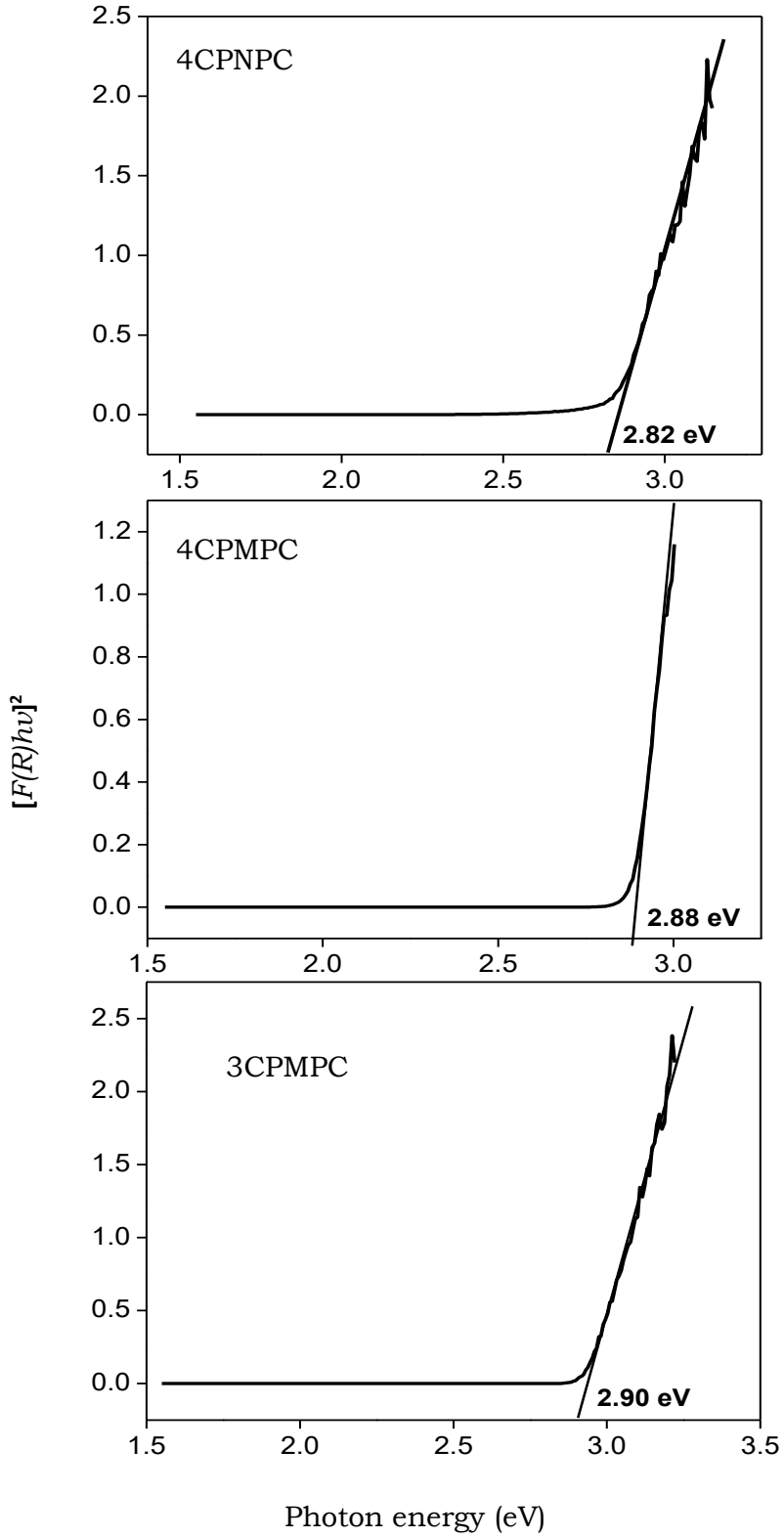

Fig. 5. Tauc plots

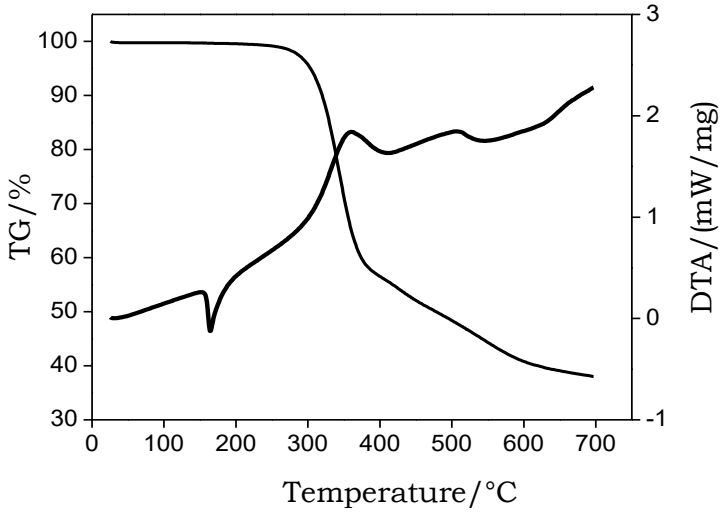

Fig. 6 (a). TG/DTA curves of

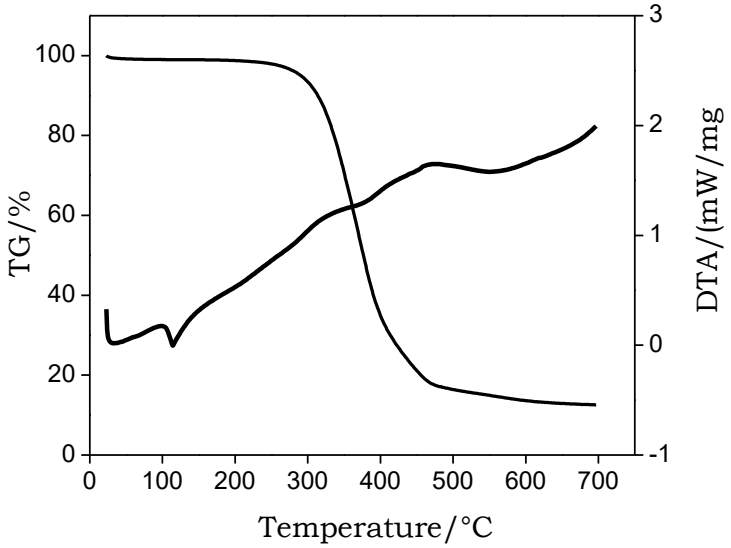

Fig. 6(b). TG/DTA curves of

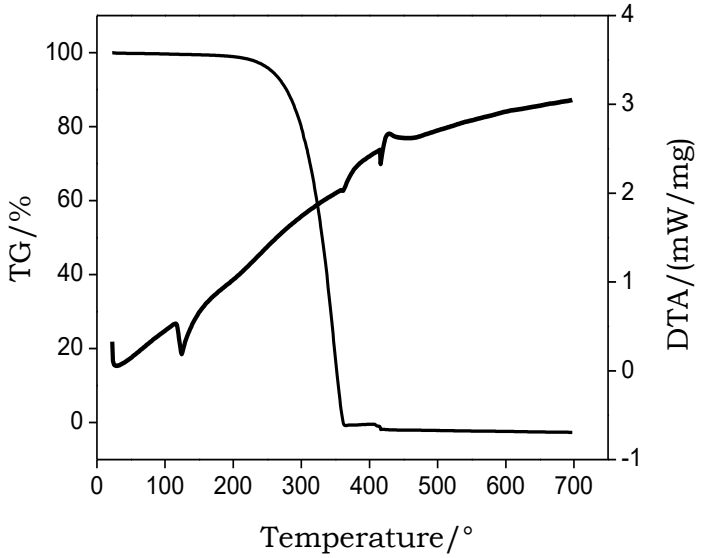

Fig. 6(c). TG/DTA curves of

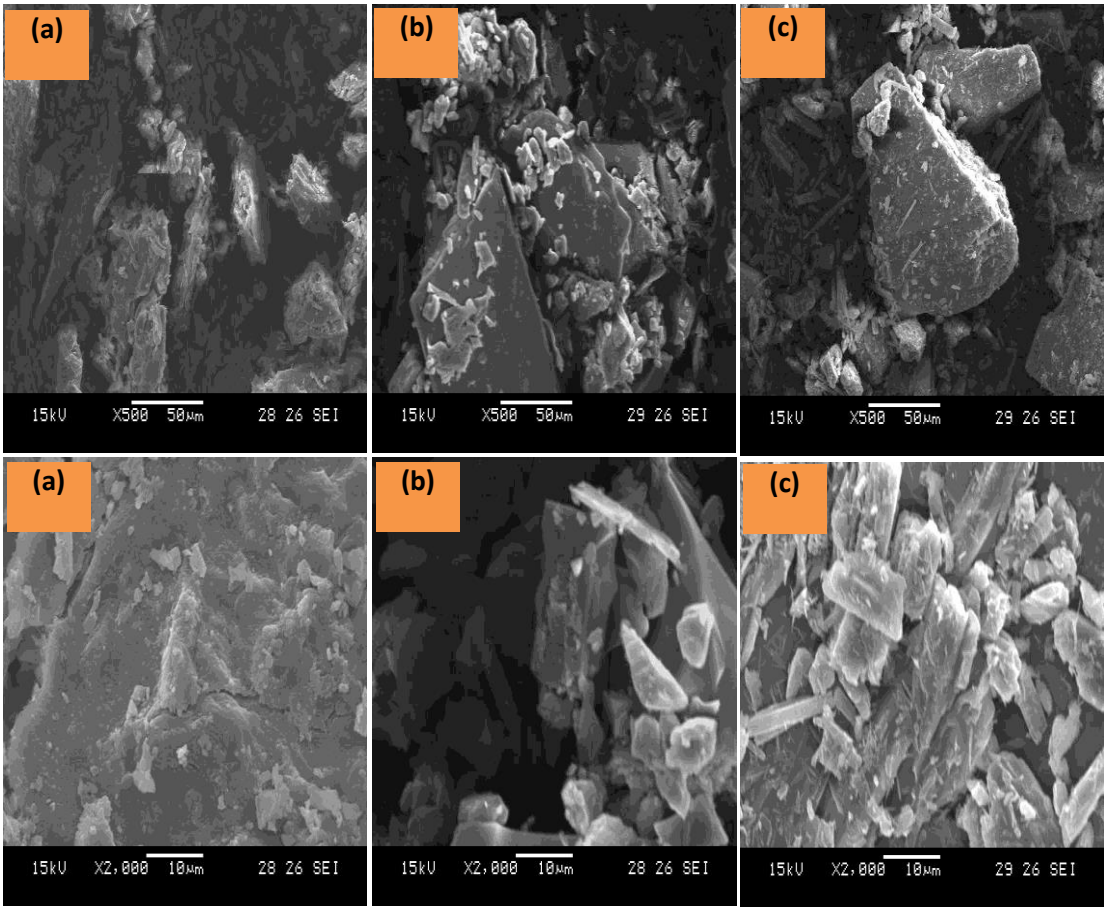

Fig. 7. SEM micrographs of (a) 4CPNPC (b) 4CPMPC and (c) 3CPMPC

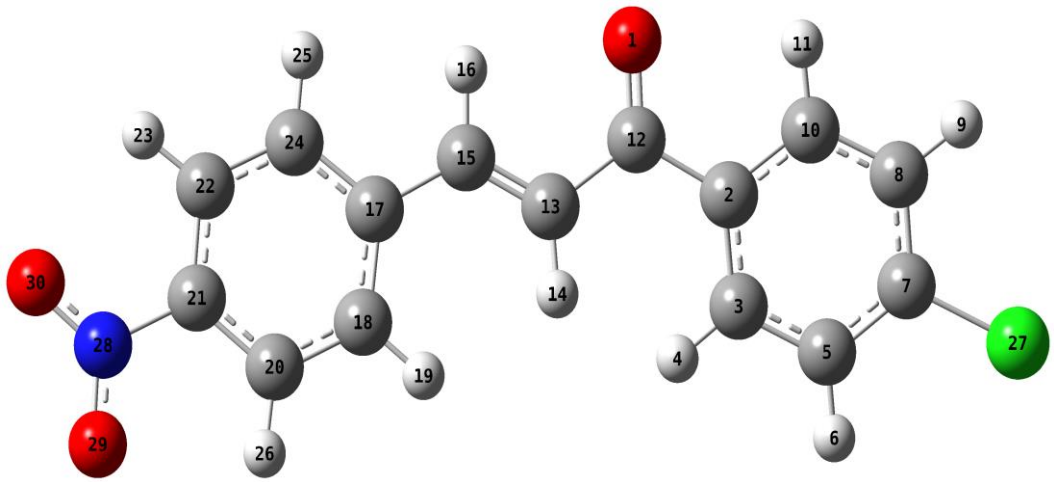

Fig. 8 (a). Optimized molecular structure of 4CPNPC

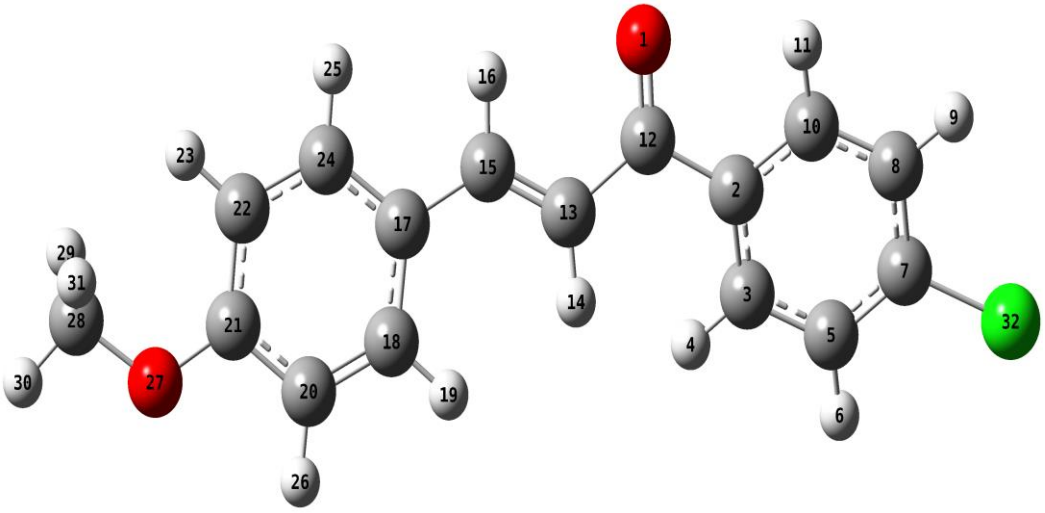

Fig. 8 (b). Optimized molecular structure of 4CPMPC

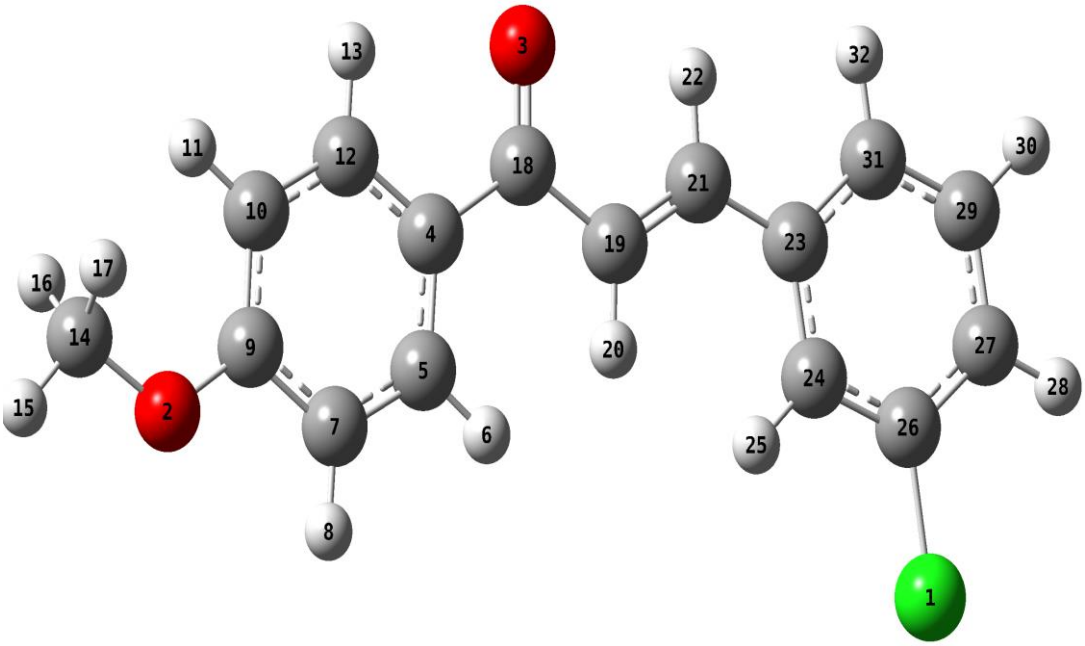

Fig. 8 (c) Optimized molecular structure of 3CPMPC

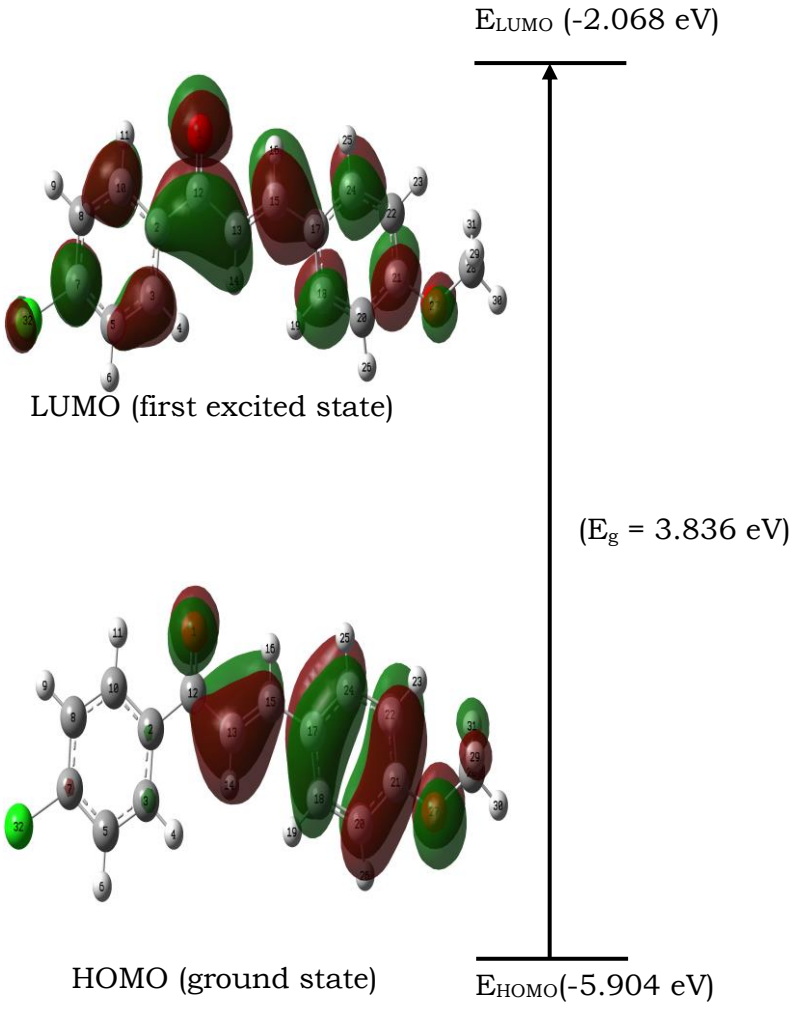

Fig. 9. Frontier molecular orbital diagram for 4CPMPC

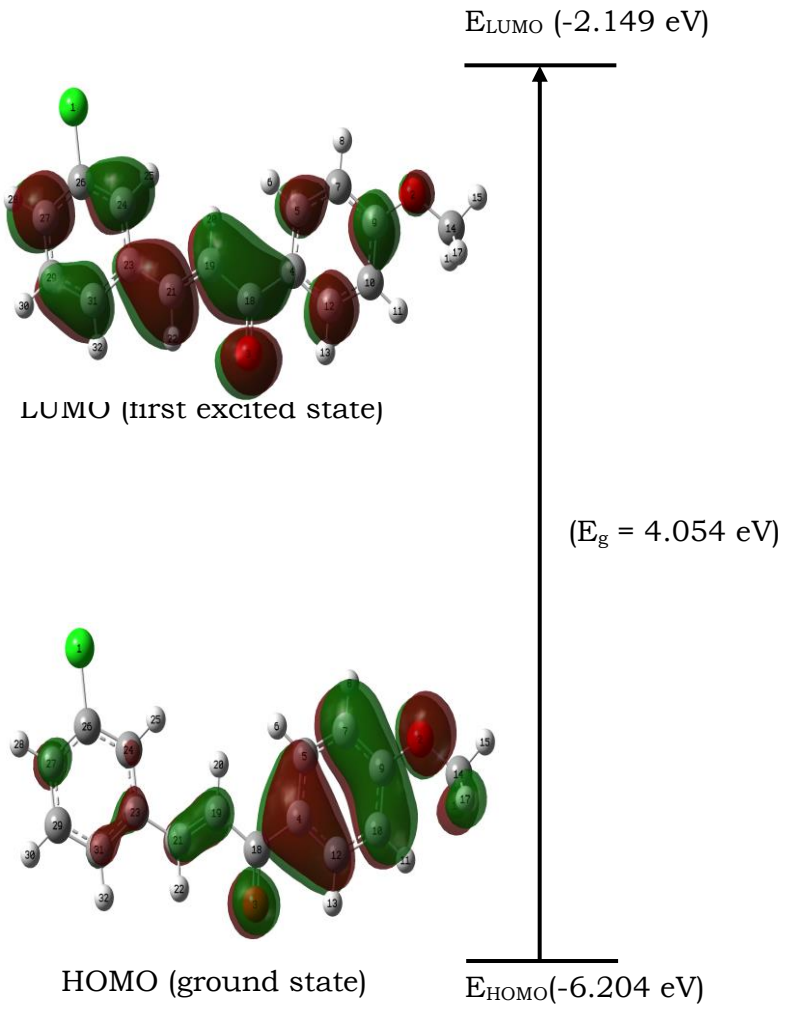

Fig. 10. Frontier molecular orbital diagram for 3CPMPC